Stability of the Heme Environment of the Nitric Oxide Synthase from *Staphylococcus aureus* in the Absence of Pterin Cofactor

François J. M. Chartier and Manon Couture
Department of Biochemistry and Microbiology, Laval University, Quebec City, Quebec, Canada

ABSTRACT We have used resonance Raman spectroscopy to probe the heme environment of a recently discovered NOS from the pathogenic bacterium *Staphylococcus aureus,* named SANOS. We detect two forms of the CO complex in the absence of L-arginine, with $\nu_{Fe\text{-}CO}$ at 482 and 497 cm^{-1} and $\nu_{C\text{-}O}$ at 1949 and 1930 cm^{-1}, respectively. Similarly to mammalian NOS, the binding of L-arginine to SANOS caused the formation of a single CO complex with $\nu_{Fe\text{-}CO}$ and $\nu_{C\text{-}O}$ frequencies at 504 and 1917 cm^{-1}, respectively, indicating that L-arginine induced an electrostatic/steric effect on the CO molecule. The addition of pterins to CO-bound SANOS modified the resonance Raman spectra only when they were added in combination with L-arginine. We found that (6R) 5,6,7,8 tetra-hydro-L-biopterin and tetrahydrofolate were not required for the stability of the reduced protein, which is 5-coordinate, and of the CO complex, which does not change with time to a form with a Soret band at 420 nm that is indicative of a change of the heme proximal coordination. Since SANOS is stable in the absence of added pterin, it suggests that the role of the pterin cofactor in the bacterial NOS may be limited to electron/proton transfer required for catalysis and may not involve maintaining the structural integrity of the protein as is the case for mammalian NOS.

INTRODUCTION

Nitric oxide synthases are heme-iron enzymes commonly found in animals and insects (Sengupta et al., 2003). The best characterized NOS are those from mammals that catalyze through two consecutive catalytic cycles the hydroxylation of L-arginine into nitric oxide and L-citrulline (Marletta, 1994). Animal NOS are homodimeric proteins and consist of an amino-terminal domain containing a heme group, a C-terminal reductase domain with FMN and FAD cofactors, and a regulatory region that control the rate of electron transfer between these two domains (Alderton et al., 2001; Marletta, 1994; Raman et al., 2000). The electrons required for the catalytic reactions are provided by NADPH and travel to the heme *via* the FMN and FAD cofactors of the reductase domain of the enzyme. Essential to the enzyme activity is a pterin cofactor, H_4B, without which the enzyme does not produce NO (Adak et al., 2000; Cosentino and Luscher, 1999; Wei et al., 2003). This pterin binds at the dimer interface, close to the heme group. H_4B forms extensive Van der Waals interactions and H-bonds with surrounding amino acids and the heme propionates, which helps stabilize the dimeric form of the enzyme (Abu-Soud et al., 1995). In all NOS characterized to date, the heme is attached to the protein moiety through an iron-thiolate coordination bond. The active site of the enzyme is composed of the heme group, the H_4B binding site, and the L-arginine binding site near the iron on the opposite side of the iron-thiolate bond.

The first description of a bacterial, L-arginine-dependent NO synthase activity has been from the bacterium *Nocardia* (Chen and Rosazza, 1994, 1995). Recently, genes encoding proteins similar to animal NOS have been found in other bacteria including *Bacillus subtilis* (Kunst et al., 1997), *Staphylococcus aureus* (Kuroda et al., 2001), and *Deinococcus radiodurans* (White et al., 1999) (Fig. 1). Bacterial NOS are particular in that they lack the reductase domain (Fig. 1) (Bird et al., 2002). Several residues near the amino-terminus are also missing (Fig. 1). In the folded animal NOS, these amino-terminal residues protect the pterin site from exposure to the solvent. Three bacterial NOS, BANOS (Adak et al., 2002a), SANOS (Bird et al., 2002), and DANOS (Adak et al., 2002b), have been expressed as recombinant proteins in *Escherichia coli*. BANOS was found to synthesize NO in single-turnover experiments when supplied with N^G-hydroxy-L-arginine and H_4B (Adak et al., 2002a), and both BANOS and DANOS were shown to synthesize nitrite under equilibrium conditions using L-arginine or N^G-hydroxy-L-arginine as substrates (Adak et al., 2002a,b). However, the turnover number was found to be very small possibly due to the use of the reductase domain of a mammalian NOS instead of the cognate reductase. It must be stressed that although the bacterial NOS are able to carry out NO synthesis in vitro, no evidence exists for such a reaction in vivo.

The crystalline structure of BANOS in complex with L-arginine (Pant et al., 2002) and that of SANOS in complex

Submitted March 8, 2004, and accepted for publication May 26, 2004.

Address reprint requests to Manon Couture, Assistant Professor, Dept. of Biochemistry and Microbiology, Pavillon Marchand, Room 4165, Laval University, Quebec City, Quebec G1K 7P4, Canada. Tel.: 418-656-2131 ext. 13515; Fax: 418-656-7176; E-mail: manon.couture@bcm.ulaval.ca.

Abbreviations used: NOS, nitric oxide synthase; NO, nitric oxide; SANOS, NOS of *Staphylococcus aureus*; BANOS, NOS of *Bacillus subtilis*; DANOS, NOS of *Deinococcus radiodurans*; nNOS, neuronal form of mammalian NOS; iNOS, inducible form of mammalian NOS; eNOS, endothelial form of mammalian NOS; H_4B, (6R) 5,6,7,8 Tetra-hydro-L-biopterin; THF, tetrahydrofolate; Fe^{3+}, ferric form; Fe^{2+}, ferrous form; CO complex, ferrous carbon monoxide form.

0006-3495/04/09/1939/12 $2.00

doi: 10.1529/biophysj.104.042119

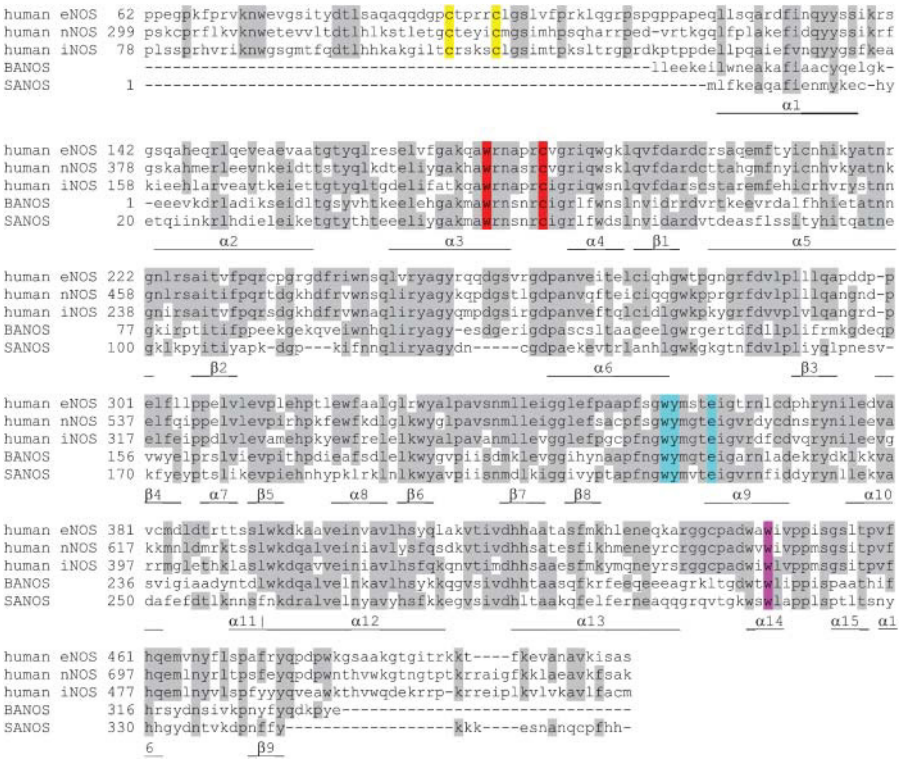

FIGURE 1 Multiple-amino acid sequence alignment of SANOS (National Center for Biotechnology Information, NP_37502) and BANOS (CAB12592) with the human iNOS (P35228), eNOS (NP_000594), and nNOS (P29475). Conserved residues in four out of six sequences at a given position are colored in gray. The two cysteine residues involved in the formation of the zinc binding site at the dimer interface of mammalian NOS are colored in yellow. The conserved cysteine residue coordinated to the heme is colored in red, as well as the tryptophan residue that forms a hydrogen bond to the sulfur group of the proximal cysteine. The cyan color is used to identify residues involved in the binding of the substrate L-arginine and a conserved tryptophan residue that forms a hydrogen bond with the pterin in mammalian NOS is colored in pink. The position of the α-helices and the β-sheets of SANOS are shown below the alignment (Bird et al., 2002). The sequences of the mammalian NOS include only the oxygenase domain; the C-terminal reductase domain is not shown. The alignment was produced with the neighbor-joining method in Clone Manager Suite (Scientific & Educational Software, Durham, NC).

with the NOS inhibitor SEITU (S-ethylisotiourea) were recently published (Bird et al., 2002). The structure showed that in SANOS, the pterin binding site is more exposed to the solvent than that of mammalian NOS because several of the N-terminal residues that protect the pterin from solvent exposure in mammalian NOS are missing. Nonetheless, the protein exists as a dimer in solution and the crystal structure revealed that the dimer is stabilized by alternative interactions (Bird et al., 2002). The pterin binding site is larger in SANOS than in mammalian NOS and is occupied by a NAD^+ molecule in the crystals. It appears that some bacteria, such as *S. aureus*, in which NOS genes have been found, may not be able to synthesize H_4B because they lack the sepiapterin reductase, the last enzyme of the biosynthetic pathway for the synthesis of H_4B (Adak et al,. 2002b; Raman et al., 2000). However, it is possible that *B. subtilis* may be able to synthesize H_4B (Adak et al., 2002a). The nature of the natural cofactor of the bacterial NOS remains to be determined.

To characterize the environment of the active site of bacterial NOS, we purified the recombinant SANOS and probed it with resonance Raman spectroscopy, which is a very powerful technique that provides a wealth of information about the structure and electronic properties of the heme group and of the heme axial ligands. We show that the binding of L-arginine to SANOS induces changes to the heme group similar to those observed in mammalian NOS. However, the binding of H_4B and THF have little structural/electronic effects on the protein and we show that these are not required for stability of the ferrous and the CO complex. Our results suggest that, in contrast to mammalian NOS, the pterin cofactor of the bacterial NOS may not have a role in the maintenance of the structural integrity of the protein although it would be required for the catalytic activity.

EXPERIMENTAL PROCEDURES

Chemicals

H_4B was from Alexis Biochemicals (San Diego, CA). Sodium dithionite was obtained from Fluka (Sigma-Aldrich, Oakville, Canada). Argon and $^{12}C^{16}O$ were from Praxair (Mississauga, Canada) .$^{13}C^{16}O$ gas was purchased from Cambridge Isotope Laboratories (Andover, MA) and $^{12}C^{18}O$ and $^{13}C^{18}O$ were from Icon Isotopes (Summit, NJ).

Protein expression and purification

The *SANOS* gene was amplified by the PCR method from *S. aureus* genomic DNA (American Type and Culture Collection (ATCC) 35556) and cloned in the pet30B expression vector (Novagen, Madison, WI) in frame with an N-terminal tag composed of six histidine residues. The cloned gene was sequenced at a local facility and found to be identical to the sequence deposited at the National Center for Biotechnology Information (NCBI) (NC_002745). The recombinant protein was expressed in *E. coli* BL21(DE3) and was purified by affinity chromatography over a Ni^{2+}-Sepharose column (Amersham Biosciences, Baie d'Urfé, Canada). Briefly, *E. coli* cells grown in Terrific Broth medium (Sambrook et al., 1989) supplemented with 10 μg/ml of kanamycin were recovered after an overnight induction by 1 mM isopropyl-β-D-thiogalactopyranoside that was added when the optical density of the culture had reached 0.8. The cells were disrupted using a French pressure cell and the cell lysate was centrifuged at

10000 × *g* for 30 min at 4°C. Ammonium sulfate precipitation was then carried out on the soluble proteins fraction. Proteins that precipitated between 35% and 50% ammonium sulfate saturation were harvested by centrifugation, resuspended in purification buffer (40 mM Hepes, pH 7.5, 150 mM NaCl, 1 mM PMSF) and loaded on a 40-ml Ni^{2+}-sepharose column. The column was washed successively with 10 column volumes of purification buffer containing 20 mM, 50 mM, and 100 mM imidazole, respectively. SANOS was eluted in purification buffer containing 400 mM imidazole. The purified protein was dialyzed at 4°C against 40 mM Hepes, pH 7.5, buffer containing 1 mM DTT, 150 mM NaCl and 10% glycerol and was kept at −80°C. The purified protein migrated with an apparent molecular weight of 42 kDa on sodium dodecyl sulfate polyacrylamide gel electrophoresis. The molecular weight in solution, determined by gel filtration over a Superdex HR200 column (Amersham Biosciences, Baie d'Urfe, Canada), was 72 kDa indicating that SANOS is a dimer in solution (the calculated molecular mass of the SANOS monomer including heme and the His-tag is 45.9 kDa). The buffer used for gel filtration chromatography was 40 mM Hepes, pH 8, 150 mM NaCl, and 1 mM DTT. The heme *b* content was quantified by the pyridine hemochrome method (Appleby, 1978).

Affinity for L-arginine

The affinity of SANOS for L-arginine was determined by the spectral changes caused by L-arginine binding to the ferric enzyme (McMillan and Masters, 1993).

Sample preparation for spectroscopy

The buffer used was 40 mM Hepes, pH 7.6, containing 1 mM DTT and 40 mM NaCl. To obtain spectrum of the ferric protein in the absence of substrate, DTT was not included in the buffer as this compound forms a low-spin complex with the heme. Where indicated, 1 mM L-arginine, 600 μM THF, and 1.2 mM H_4B were added to the protein samples.

Optical spectroscopy

Optical spectra were recorded with a Cary 3 spectrophotometer with samples placed in a 1-cm path-length anaerobic cuvette (Hellma, Müllheim, Germany). The Fe^{2+} sample was prepared by equilibration of the sample solution with argon followed by the addition of a small volume of a freshly prepared anaerobic solution of sodium dithionite. The CO complexes were prepared by incubating the protein samples with argon, adding a known volume of CO gas, and reducing the heme with a small amount of freshly prepared sodium dithionite. The protein concentration was 5 μM.

Resonance Raman spectroscopy

To obtain resonance Raman spectra, the 441.6 nm line of an He/Cd laser (Liconix laser, Melles-Griot, Canada) was used to probe CO complexes, and the 406 and 413 lines of a Kr-ion laser (Innova 302 Kr laser, Coherent, Santa Clara, CA) were used to probe ferric and ferrous forms of SANOS. The laser beam was focused to an ~55 μM spot on a custom-made sample cuvette, which was kept rotating at 1000 rpm to avoid local heating of the sample. The scattered light was collected at a 90° angle with an F#1 lens and refocused with an F#9.8 lens on the entrance slit of a 0.75-m spectrograph (Acton Research, Acton, MA) equipped with an 1800 lines/mm diffraction grating. A Notch filter, designed to block light at 441.6 nm (MK Photonics, Albuquerque, NM) or at 406 and 413 nm (Kaiser Optical, Ann Arbor, MI) was placed in front of the entrance slit of the spectrometer to prevent Rayleigh scattered light from entering the spectrometer. The width of the spectrometer slit was set at 100 microns. The diffracted light was detected at the spectrometer exit with a liquid nitrogen-cooled CCD camera (Spec10:100B, Roper Scientific, Trenton, NJ). Cosmic rays were automatically removed from spectra by a software routine of WinSpec (Roper Scientific). Typically, several 1-min spectra were recorded with a low excitation power, 1.4–4.8 mW, at room temperature and averaged with the Grams software (ThermoGalactic, Salem, NH). The spectra were calibrated with the lines of indene in the 200–1700 cm^{-1} region and with the lines of acetone and potassium ferrocyanide in the 1600–2100 cm^{-1} region. To verify the stability of the samples, optical spectra of the samples in the Raman cuvette were recorded before and after resonance Raman spectra were obtained. Typically, samples containing 30–40 μM protein, based on the heme content, were used to acquire the resonance Raman spectra. To obtain the resonance Raman spectra of ferrous SANOS in the perpendicular and parallel orientations, a polarizer (Newport, Irvine, CA) in combination with a polarization scrambler was placed in front of the entrance slit of the spectrometer. The efficiency of this setup was verified by measuring the polarization ratio of the 460 cm^{-1} line of CCl_4.

RESULTS

Optical spectra of SANOS

The SANOS protein was expressed in *E. coli* and was purified in the absence of added pterin and substrate L-arginine. The purified protein displayed an optical spectrum with a large Soret band with maxima at 395 nm and 418 nm, respectively, suggesting a mixture of high-spin and low-spin hemes (spectrum not shown). The addition of L-arginine to the SANOS sample caused the disappearance of the 418-nm band and the resulting spectrum was typical of those of 5-coordinate, high-spin heme proteins with a Soret band centered at 398 nm (Fig. 2). The identity of the natural cofactor of SANOS is unknown. We used here H_4B and THF, a pterin analog that was showed to support NO synthesis in DANOS (Adak et al., 2002b). The addition of H_4B or THF to SANOS changed the optical spectrum of the

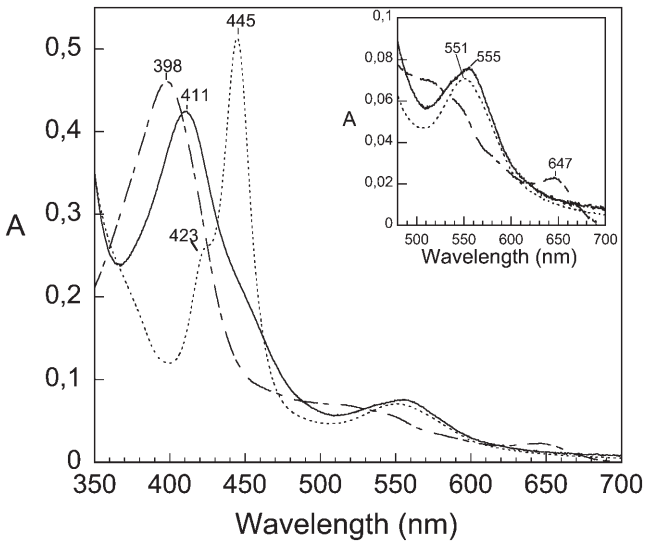

FIGURE 2 Optical absorption spectra of the purified SANOS. The spectra shown are those of the ferric protein saturated with L-arginine (*slotted line*), the ferrous protein (*continuous line*), and the CO complex (*dotted line*). The spectra of the ferrous form and of the CO complex were obtained in the absence of substrate and cofactor. The inset shows an enlarged portion of the visible region. The protein concentration was 5 μM.

ferric enzyme and we observed an increase of the intensity of the band at 398 nm and a diminution of the intensity at 418 nm (not shown). This behavior is similar to that of mammalian NOS, which display a shift from a mixture of 5-coordinate and 6-coordinate forms to a 5-coordinate, high-spin form with a Soret band near 397 nm when saturated with H_4B (Ghosh et al., 1997). These spectral changes caused by the addition of H_4B or THF alone to SANOS indicate that these molecules bind to the protein and that they induce a shift in the heme coordination state similar to that of the mammalian NOS.

Upon reduction of the ferric form (Fig. 2), the ferrous SANOS displayed a Soret band centered at 411 nm, suggesting that the heme is 5-coordinate and high-spin (Wang et al., 1993). Addition of CO to the ferrous protein shifted the Soret band to 445 nm with a minor contribution near 423 nm (Fig. 2). For the CO complex of NOS and P450, a Soret band near 450 nm indicates that the heme forms an iron-thiolate bond on the proximal side whereas a Soret band near 420 nm is indicative of a protein in an inactive state called P420 (Wang et al., 1995; Wells et al., 1992). For $P450_{cam}$, the proximal ligand of the P420 form was shown to be a histidine residue (Wells et al., 1992). No change in the optical spectrum of the CO complex of SANOS was observed upon addition of L-arginine, confirming that the majority of the protein is already in a native-like conformation with a cysteine residue as the proximal ligand to the heme. In contrast to the situation observed for the mammalian NOS (Wang et al., 1995), the CO complex of SANOS is very stable in the absence of pterin and substrate and no significant increase in the content of the P420 form was observed over the course of a 24-h incubation at room temperature (not shown). Under the same conditions, nNOS and iNOS convert to the P420 form with time (Wang et al., 1995).

Resonance Raman spectra of ferric SANOS

The high-frequency region of the resonance Raman spectra of heme proteins (1300–1700 cm^{-1}) contains in-plane vibrational modes of the porphyrin ring that are sensitive to the oxidation, coordination, and spin state of the heme iron (Hu et al., 1996; Spiro and Li, 1988; Wang et al., 1996). In particular, the ν_4 mode is sensitive to the electron density of the porphyrin ring and the ν_2 and ν_3 modes are sensitive to the coordination and spin state of the heme iron (Spiro and Li, 1988; Wang et al., 1996). The assignment of the coordination and spin state of ferric SANOS was obtained from the resonance Raman spectra of the substrate-free and L-arginine-bound enzyme recorded in the high-frequency region (Fig. 3). The frequencies of the ν_4 line at 1373 cm^{-1} for the substrate-free (Fig. 3 *B*) and at 1369 cm^{-1} for the L-arginine-bound protein (Fig. 3 *C*), respectively, are typical of oxidized heme proteins. Two ν_3 lines, at 1489 and 1503 cm^{-1}, respectively, were identified in the spectrum of the substrate-free SANOS (Fig. 3 *B*), indicating a mixture of

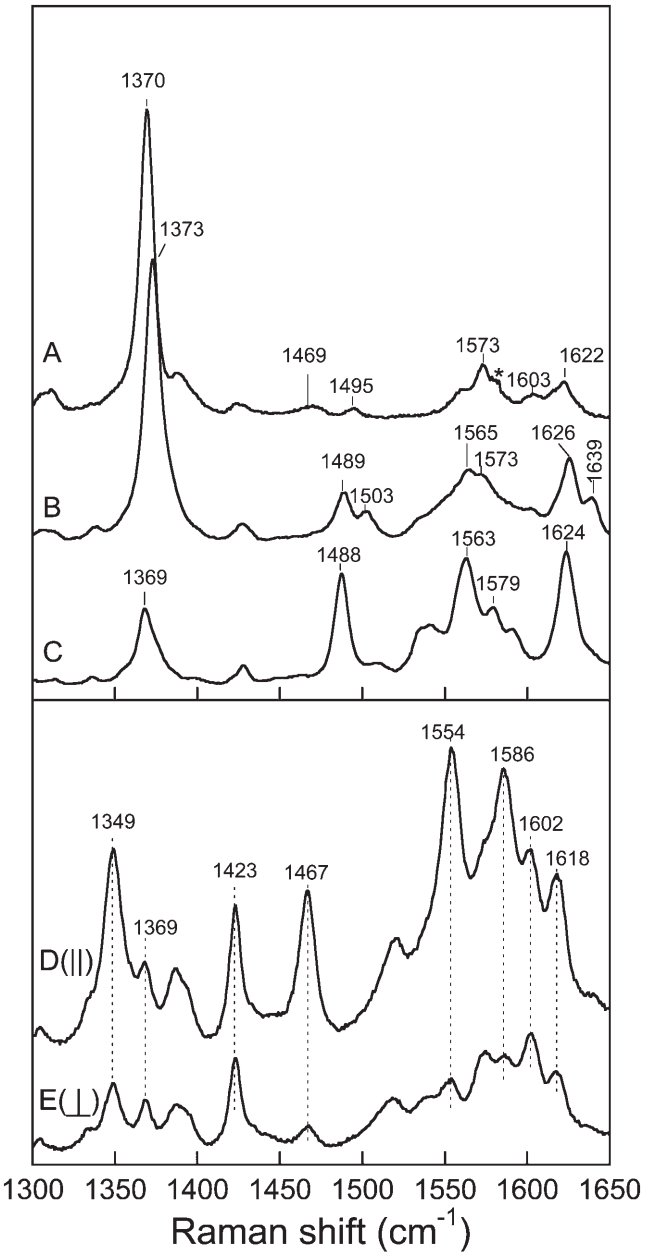

FIGURE 3 High-frequency resonance Raman spectra of SANOS. (*A*) CO complex; (*B*) substrate-free and pterin-free ferric form; (*C*) pterin-free ferric form in the presence of L-arginine; (*D*) substrate-free and pterin-free ferrous form (spectrum obtained in the parallel orientation); and (*E*) substrate-free and pterin-free ferrous form (spectrum obtained in the perpendicular orientation). The spectra were recorded with a laser line at 442 nm (*A*) and 413 nm (*B–E*) with a laser power <5 mW. The line marked by the asterisk corresponds to a line from the laser.

5-coordinate and high-spin (1489 cm^{-1}) and 6-coordinate and low-spin (1503 cm^{-1}) ferric hemes. Upon the addition of L-arginine, a single ν_3 line is observed at 1488 cm^{-1} (Fig. 3 *C*), indicating that the heme is totally 5-coordinate and high-spin. In the latter spectrum, the identification of the ν_2 line at 1563 cm^{-1} confirms this assignment. The assignment of the ν_2 line of the substrate-free protein was not possible because

this region of the spectrum is complicated by the presence of additional heme modes (Fig. 3 *B*).

Other heme modes are of interest, for instance, the ν_{10} mode that is usually observed near 1638 cm^{-1} in the spectra of 6-coordinate and low-spin ferric heme proteins. For SANOS, the ν_{10} mode is observed at 1639 cm^{-1} (Fig. 3 *B*). As reported for eNOS (Schelvis et al., 2002) and nNOS (Wang et al., 1995), the ν_{10} mode of the 5-coordinate and high-spin form of SANOS convolutes with the $\nu_{C\text{-}C}$ vinyl stretching mode at 1624 cm^{-1}. A single ν_{10}/ν_{vinyl} stretching mode was identified in the presence (1624 cm^{-1}) or absence (1626 cm^{-1}) of L-arginine (Fig. 3, *B* and *C*). The nearly identical frequencies indicate that the binding of L-arginine does not induce a significant change in the orientation and/or environment of the vinyl groups. A similar behavior has been reported for the mammalian eNOS (Schelvis et al., 2002).

Resonance Raman spectra of ferrous SANOS

The high-frequency region of the resonance Raman spectrum of the ferrous form of substrate-free and pterin-free SANOS is showed in Fig. 3 *D*. The ν_4 and ν_3 lines are found at 1349 cm^{-1} and 1467 cm^{-1}, respectively, showing that the heme is 5-coordinate and high-spin. The low-frequency of the ν_4 mode is similar to the frequencies of the ν_4 modes of P450 (Champion et al., 1978) and nNOS (Wang et al., 1995) and is indicative of an iron-thiolate coordination. Other heme proteins with histidine-iron coordination have a ν_4 line at higher frequency, near 1355 cm^{-1}. The heme coordination and spin state of the ferrous SANOS did not change upon L-arginine binding (results not shown), and the heme thus remained 5-coordinate and high-spin. In contrast, ferrous nNOS is mostly 6-coordinate and low-spin in the absence of pterin and 5-coordinate and high-spin in the presence of H_4B (Wang et al., 1995). The ν_{10}/ν_{vinyl} region of ferrous SANOS, with lines at 1602 and 1619 cm^{-1} (Fig. 3 *D*), is similar to that of nNOS/H_4B with lines at 1600 and 1617 cm^{-1} (Table 1). The ferrous, H_4B-depleted nNOS, representing the P420 form, displays a single ν_{10}/ν_{vinyl} mode at 1615 cm^{-1} (Table 1) (Wang et al., 1995). The similarity of the ferrous spectrum of SANOS with that of nNOS/H_4B is a further indication that very little inactive P420 form is present in our protein preparation.

A line at 1369 cm^{-1}, not seen in the resonance Raman spectrum of reduced nNOS (Wang et al., 1993), is present in the reduced spectrum of SANOS (Fig. 3 *D*). As discussed above, it is unlikely that this line corresponds to the ν_4 line of a P420 form; moreover, the ν_4 line of such a P420 form would be expected near 1361 cm^{-1} based on the frequency observed for the ferrous P420 form of P450 (Wells et al., 1992) and nNOS (Wang et al., 1995). The 1369 cm^{-1} line also does not arise from the ν_4 line of oxidized heme. First, the optical spectrum of the ferrous sample used to obtain the Raman spectrum was verified to rule out the possibility that the sample oxidized during data acquisition. Second, the ν_4 line of the substrate-free ferric enzyme is actually at a higher frequency, 1373 cm^{-1} (Fig. 3 *B*). Measurement of the polarization sensitivity of ferrous SANOS revealed that the 1369 cm^{-1} line is not polarized, with a polarization ratio of

TABLE 1 Summary of the coordination and spin state assignment of ferric and ferrous NOS and P450

Form	Coordination	ν_4 (cm^{-1})	ν_3 (cm^{-1})	ν_{10}/ν_{vinyl} (cm^{-1})	Reference
Fe^{3+} SANOS[a]	5C HS	1373	1489	1626	A
Fe^{3+} SANOS/Arg*	6C LS	1373	1503	1639	A
Fe^{3+} nNOS/H_4B	5C HS	1369	1488	1624	B
Fe^{3+} nNOS (no pterin)	5C HS	1370	1488	1623	B
Fe^{3+} eNOS/H_4B	5C HS	1371	1487	1623	C
Fe^{3+} $P450_{cam}$	6C LS	1371	1502	n.d.	D
$Fe^{3+}P450_{cam}$/camphor	5C HS	1370	1488	n.d.	D
	6C LS	1373	1500	1638	
	6C LS	1373	1503	1635	
	5C HS	1368	1488	1623	
	6C LS	1372	n.d.	1637	
Fe^{2+} SANOS	5C HS	1349	1467	1602/1619	A
Fe^{2+} SANOS/Arg	5C HS	1349	1467	1602/1619	A
Fe^{2+} nNOS/H_4B	5C HS	1347	1466	1600/1617[†]	B
Fe^{2+} nNOS (no pterin) (420 form)	6C LS	1360(sh)	1490	1615	B
	6C LS	1360	1467		
	5C HS	n.d.			

In ''Reference'' column, *A*, this work; *B*, Wang et al., 1995; *C*, Rodriguez-Crespo et al., 1997; and *D*, Wells et al., 1992. n.d., not determined; sh, shoulder.
*We also obtained the spectrum of ferric SANOS/H_4B. The heme is mostly 5-coordinate and high-spin as we detect only the ν_3 line at 1489 cm^{-1}. However, the quality of the spectrum is poor due to fluorescence of the sample caused by H_4B.
[†]The values were not specifically assigned to the 5-coordinate or the 6-coordinate form.

0.99, in contrast to the ν_4 line at 1349 cm^{-1} that displays a polarization ratio of 0.28 (Fig. 3, *D* and *E*). This result establishes that the 1369 cm^{-1} arises from a heme mode other than ν_4, and therefore we conclude that ferrous SANOS is 5-coordinate and high-spin in the presence or absence of L-arginine and pterins with no other detectable form.

Resonance Raman spectra of the CO complexes

CO is widely used to probe the active site of heme proteins because it produces a very stable heme complex and because it is a sensitive probe of electronic and steric interactions within the heme pocket (Aono et al., 2002; Couture et al., 2001; Fan et al., 1997; Igarashi et al., 2003; Mukai et al., 2002; Phillips et al., 1999; Uchida et al., 1998; Wang et al., 1997). In the high-frequency region of the resonance Raman spectrum of the CO complex (Fig. 3 *A*), the ν_4 line and the ν_3 line are identified at 1370 and 1495 cm^{-1}, respectively, revealing that the complex is 6-coordinate and low-spin. No significant photodissociation of the heme-bound CO molecule occurred during spectral acquisition as indicated by the absence of the ν_4 line (1349 cm^{-1}) and of the ν_3 line (1467 cm^{-1}) of the 5-coordinate, high-spin ferrous form. In contrast, these two lines are present in the resonance Raman spectrum of the CO complex acquired at high laser power (~50 mW; results not shown).

CO isotopes were used to identify the $\nu_{Fe\text{-}CO}$ and $\delta_{Fe\text{-}C\text{-}O}$ modes in the low-frequency region of the resonance Raman spectra. The spectra of the substrate-free enzyme were recorded first. Fig. 4 shows an isotope-sensitive line located approximately at 489 cm^{-1} that shifts monotonously in going from $^{12}C^{16}O$ (Fig. 4 *D*), to $^{13}C^{16}O$ (Fig. 4 *C*), to $^{12}C^{18}O$ (Fig. 4 *B*), and to $^{13}C^{18}O$ (Fig. 4 *A*). This behavior is expected for the $\nu_{Fe\text{-}CO}$ stretching mode of a CO complex and has been observed for many heme proteins (Wang et al., 1997; Yu et al., 1984). The isotope sensitive line at ~489 cm^{-1}, which is quite large (with a width at half-height of 35 cm^{-1}), was further investigated by spectral deconvolution. For the $^{12}C^{16}O$ spectrum, two lines, at 482 and 497 cm^{-1}, respectively, with approximately the same area under the curve, were deconvoluted (not shown). In contrast, the $^{13}C^{18}O$ spectrum revealed two major lines at 470 cm^{-1} and 481 cm^{-1} and a smaller intensity line at 498 cm^{-1} (Fig. 4, *inset*). Since the line at 498 cm^{-1} is not shifting with the different CO isotopes, the latter was assigned to a heme mode. We conclude that the 497 cm^{-1} line deconvoluted from the $^{12}C^{16}O$ spectrum is composed of a small-intensity heme mode at 498 cm^{-1} and of a larger-intensity line at 497 cm^{-1} that we assign to a $\nu_{Fe\text{-}CO}$ mode. SANOS thus displays two $\nu_{Fe\text{-}CO}$ modes located at 482 cm^{-1} and 497 cm^{-1}, respectively, with $^{12}C^{16}O$. These lines shift to 470 cm^{-1} and 481 cm^{-1}, respectively, with $^{13}C^{18}O$. The magnitude of the $^{12}C^{16}O - {}^{13}C^{18}O$ isotope shift of the 497 cm^{-1} mode, 16 cm^{-1}, corresponds to the value expected for a system behaving as a diatomic oscillator and the magnitude of the isotope shift of the 482 cm^{-1} line, 12 cm^{-1}, is smaller than the expected shift but is similar to that observed in nNOS (Wang et al., 1997) (Table 2).

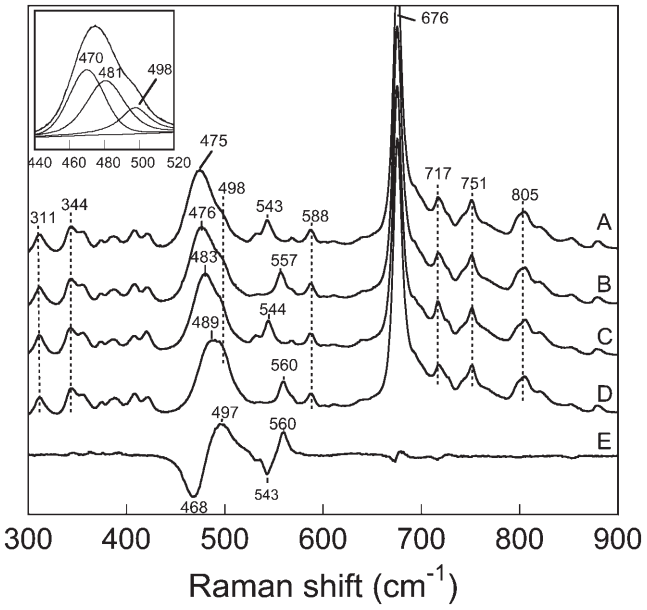

FIGURE 4 Low-frequency region of the resonance Raman spectra of the CO complex of SANOS in the absence of L-arginine and pterin. Samples were prepared with $^{13}C^{18}O$ (*A*), $^{12}C^{18}O$ (*B*), $^{13}C^{16}O$ (*C*), and $^{12}C^{16}O$ (*D*). The $^{12}C^{16}O - {}^{13}C^{18}O$ difference spectrum is shown in (*E*). The inset shows the results of the deconvolution of the ~475 cm^{-1} region of spectrum *A*.

A third line at 560 cm^{-1} (Fig. 4 *D*) displayed isotope sensitivity with shifts to 544 cm^{-1}, 557 cm^{-1}, and 543 cm^{-1} with $^{13}C^{16}O$, $^{12}C^{18}O$, and $^{13}C^{18}O$, respectively. This line was assigned to the $\delta_{Fe\text{-}C\text{-}O}$ bending mode of SANOS as it displayed the typical zigzag pattern of the $\delta_{Fe\text{-}C\text{-}O}$ bending mode of heme proteins (Yu et al., 1984).

To identify the $\nu_{C\text{-}O}$ stretching mode of substrate-free SANOS, the resonance Raman spectra were recorded in the 1600–2100 cm^{-1} region (Fig. 5, *A–C*). Two lines, at 1949 cm^{-1} and 1930 cm^{-1}, respectively, that shifted to 1857 cm^{-1} and 1843 cm^{-1}, respectively, with $^{13}C^{18}O$, were assigned to two $\nu_{C\text{-}O}$ stretching modes as they fall in the region observed for the $\nu_{C\text{-}O}$ stretching modes of other heme proteins (Table 2). The magnitude of the isotope shifts, 92 cm^{-1} and 87 cm^{-1}, respectively, corresponds well to the theoretical value expected for a diatomic oscillator (91 cm^{-1}). Based on the reversed relationship displayed by the frequencies of the $\nu_{Fe\text{-}CO}$ and $\nu_{C\text{-}O}$ modes (Li and Spiro, 1988; Ray et al., 1994; Vogel et al., 2000), we propose the existence of two CO complexes of SANOS: one is characterized by the 1930 cm^{-1} $\nu_{C\text{-}O}$ mode and the $\nu_{Fe\text{-}CO}$ mode at 497 cm^{-1} whereas the second is characterized by the 1949 cm^{-1} $\nu_{C\text{-}O}$ mode and the $\nu_{Fe\text{-}CO}$ mode at 482 cm^{-1}. As shown in Fig. 7, a plot of the $\nu_{Fe\text{-}CO}$ versus $\nu_{C\text{-}O}$ frequencies shows that the modes for SANOS, open circles 1 and 2, fall in the region of heme proteins having thiolate coordination.

TABLE 2 Frequencies of the $\nu_{Fe\text{-}CO}$ and $\nu_{C\text{-}O}$ lines of various NOS, $P450_{cam}$, and chloroperoxidase (CPO)

Protein	No.	Frequency (cm^{-1}) $\nu_{Fe\text{-}CO}$ ($^{13}C^{18}O$)	$\delta_{Fe\text{-}C\text{-}O}$ ($^{13}C^{18}O$)	$\nu_{C\text{-}O}$ ($^{13}C^{18}O$)	Reference
SANOS	1	482 (470)*	560 (543)†	1949 (1857)‡	This work
	2	497 (481)*		1930 (1843)‡	
SANOS/Arg	3	504 (496)	567 (548)	1917 (1830)	This work
nNOS/H_4B	4	487 (~477)	562 (544)	1949 (1856)	A
	5	501 (~491)		1930 (1837)	
nNOS/H_4B/Arg	6	503 (493)	565 (546)	1929 (1841)	A
iNOS/H_4B		479¶	560 (550)	1945 (1846)§	B
		499¶			
iNOS/H_4B/Arg	7	512 (499)	567 (551)	1906 (1819)	B
eNOS/H_4B/Arg		512	567	N.D.	B
$P450_{cam}$ (substrate-free)	8	464	556	1963	C
$P450_{cam}$/camphor	9	481	558	1940	C
CPO pH 6.1	14	485 (474)	560 (538)	1957.5 (1872)	A

Numbers in ''No.'' column refer to data points in Fig. 7. In ''Reference'' column, *A*, Wang et al. (1997); *B*, Fan et al. (1997); *C*, Uno et al. (1985) and Wells et al. (1992).

*The best fit to the data for the deconvolution of the broad 489 cm^{-1} band with $^{12}C^{16}O$ identifies a line at 482 cm^{-1} that we assign to a $\nu_{Fe\text{-}CO}$ mode and a line at 497 cm^{-1} that we assign as a $\nu_{Fe\text{-}CO}$ mode plus a less intense heme mode at 498 cm^{-1}. This assignment is confirmed with deconvolution of the $^{13}C^{18}O$ spectrum where the broad line centered at 475 cm^{-1} is resolved in two $\nu_{Fe\text{-}CO}$ at 470 cm^{-1} and 481 cm^{-1}, respectively, and a heme mode at 498 cm^{-1}.

†The bending mode is not assigned to one set of $\nu_{Fe\text{-}CO}$ and $\nu_{C\text{-}O}$ modes or the other.

‡The precise position of the bands was obtained from spectral deconvolution.

¶The undeconvoluted $\nu_{Fe\text{-}CO}$ line is centered at 487 cm^{-1} and shifts to 474 cm^{-1} with $^{13}C^{18}O$.

§Broad band.

L-arginine and cofactors binding

The effect of L-arginine binding to SANOS was then investigated. For this, the low-frequency region of the resonance Raman spectrum of the CO complex was recorded in the presence of a saturating amount of L-arginine. As shown in Fig. 6, *C–E*, a single line at 504 cm^{-1} displayed a shift to 496 cm^{-1} with $^{13}C^{18}O$. The frequency of this line is similar to that of the $\nu_{Fe\text{-}CO}$ mode of substrate-bound nNOS (Table 2) and is therefore assigned to the $\nu_{Fe\text{-}CO}$ mode of L-arginine-bound SANOS. The isotope shift of 8 cm^{-1} is smaller than expected but is similar to that of nNOS (Table 2). Thus the two $\nu_{Fe\text{-}CO}$ modes detected in the absence of L-arginine are replaced in the L-arginine-bound SANOS by a single $\nu_{Fe\text{-}CO}$ mode at higher frequency. The bending mode of the CO complex of L-arginine-bound SANOS is also found at a higher frequency, 567 cm^{-1} (Fig. 6 *D*), than that of the CO complex of L-arginine-free SANOS, 560 cm^{-1} (Fig. 4 *D*, Table 2).

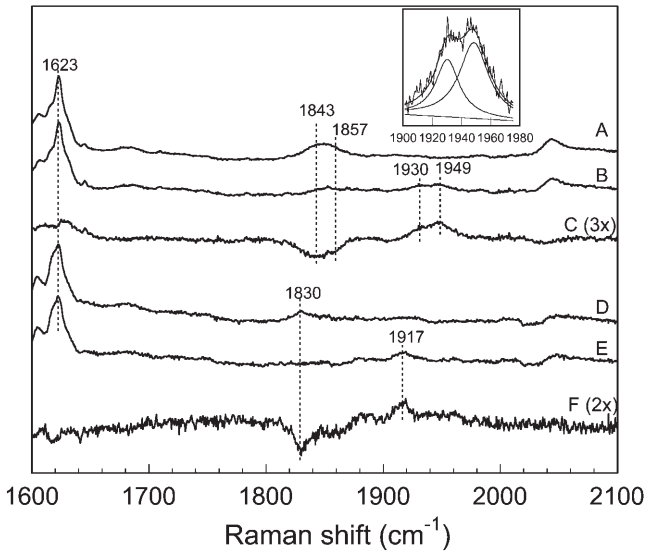

FIGURE 5 Resonance Raman spectra of the CO complex of SANOS in the $\nu_{C\text{-}O}$ region. Spectra *A–C* were obtained in the absence of L-arginine whereas spectra *D–F* were obtained in the presence of 1 mM L-arginine. (*A*) $^{13}C^{18}O$; (*B*) $^{12}C^{16}O$; (*C*) $^{12}C^{16}O - {}^{13}C^{18}O$ (3× expansion); (*D*) $^{13}C^{18}O$; (*E*) $^{12}C^{16}O$; and (*F*) $^{12}C^{16}O$ minus $^{13}C^{18}O$ difference spectrum (2× expansion). The inset shows the deconvolution of the $\nu_{C\text{-}O}$ region from spectrum *B*.

In the $\nu_{C\text{-}O}$ region of the CO spectrum of L-arginine-bound SANOS, a single isotope-sensitive line was detected at 1917 cm^{-1} with $^{12}C^{16}O$ and at 1830 cm^{-1} with $^{13}C^{18}O$ (Fig. 5). This line falls in the region where the $\nu_{C\text{-}O}$ modes of other heme proteins occur (Table 2) and it displayed an isotopic shift, 87 cm^{-1}, close to the theoretical value expected for a diatomic oscillator, 90 cm^{-1}. It is therefore assigned to the $\nu_{C\text{-}O}$ stretching mode of the CO complex of L-arginine-bound SANOS. Thus, the two $\nu_{C\text{-}O}$ stretching modes observed at 1930 and 1949 cm^{-1}, respectively, with the L-arginine-free enzyme are replaced by a single $\nu_{C\text{-}O}$ mode at 1917 cm^{-1} upon L-arginine binding (Table 2).

Inspection of the resonance Raman spectra of the L-arginine-bound enzyme (Fig. 6 *D*) and the L-arginine-free enzyme (Fig. 4 *D*) indicated that binding of L-arginine caused several changes to the resonance Raman spectrum of the CO complex. These differences are best seen in the difference spectrum calculated from the spectrum of the L-arginine-bound enzyme minus that of the substrate-free

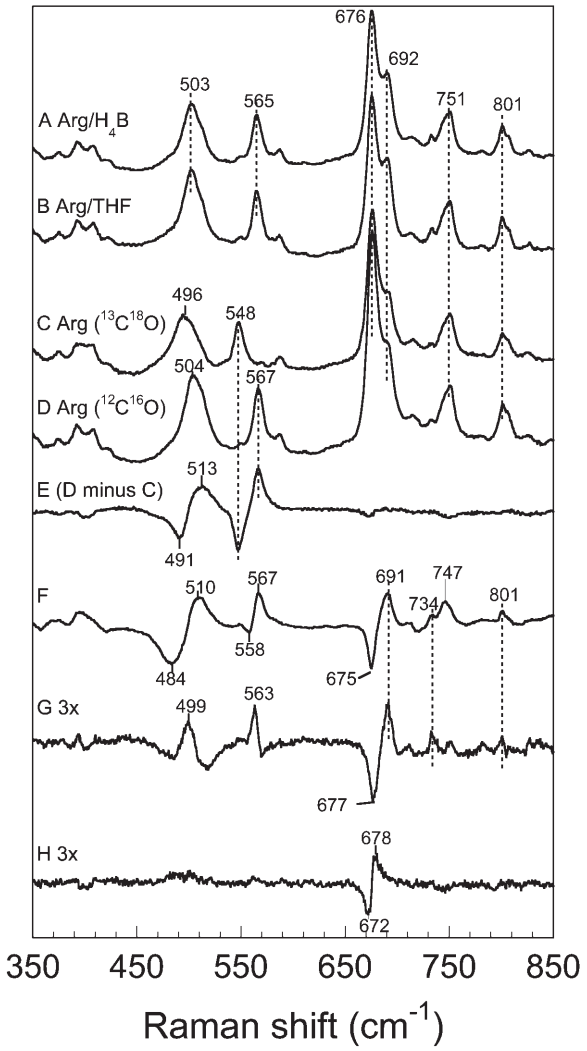

FIGURE 6 Resonance Raman spectra in the low-frequency region of the CO complex in the presence of substrate and cofactors. Spectra were recorded from samples prepared with (*A*) $^{12}C^{16}O$ in the presence of L-arginine (1 mM) and H_4B (1.2 mM); (*B*) $^{12}C^{16}O$ in the presence of L-arginine (1 mM) and THF (600 μM); (*C*) $^{13}C^{18}O$ and L-arginine (1 mM); and (*D*) $^{12}C^{16}O$ and L-arginine (1 mM). The spectrum shown in (*E*) is the $^{12}C^{16}O$ minus $^{13}C^{18}O$ difference spectrum of L-arginine-bound enzyme (*D* minus *C*). Shown in *F* is the difference spectrum between the L-arginine-containing sample and the substrate-free/pterin-free enzyme (*D* minus spectrum *D* of Fig. 4). The spectrum shown in *G* is the L-arginine/H_4B sample minus the L-arginine containing sample (*A* minus *D*). Finally, the spectrum *H* corresponds to the H_4B-containing sample (1.2 mM, not shown) minus that of the substrate-free and H_4B-free sample (spectrum *D* of Fig. 4).

enzyme (Fig. 6 *F*). Among these, the most significant changes are new maxima at 691 cm^{-1} and 734 cm^{-1}, an increase of the intensity of lines near 747 and 801 cm^{-1}, as well as a narrowing of the $\nu_{Fe\text{-}CO}$ region that is revealed by the decrease in intensity near 484 cm^{-1}. Based on the assignment of heme modes of myoglobin (Hu et al., 1996), the line at 747 cm^{-1} may correspond to the ν_{15} pyrrole breathing mode whereas the line at 801 cm^{-1} may correspond to ν_6, a heme ruffling mode. These changes at 747 and 801 cm^{-1} reveal that the heme itself undergoes structural and electronic modifications after the binding of L-arginine. In contrast, the binding of H_4B alone does not perturb the spectrum of the CO complex as shown by the difference spectrum calculated between the H_4B-saturated enzyme and the H_4B-free protein (Fig. 6 *H*) that displayed only a small imbalance of the intense line at 676 cm^{-1}. THF alone did not change the spectrum either (results not shown). However, the addition of H_4B (Fig. 6 *A*) or THF (Fig. 6 *B*) in combination with L-arginine revealed changes in the intensity and position of several heme modes. This is best observed in the difference spectrum calculated from the spectrum of the L-arginine/H_4B sample minus the spectrum of the L-arginine saturated sample (Fig. 6 *G*). For instance, there is an increase of the intensity in the $\nu_{Fe\text{-}CO}$ mode at 499 cm^{-1}, of the bending mode at 563 cm^{-1}, and other small changes to heme modes in the 700–800 cm^{-1} region.

DISCUSSION

Bacterial genes encoding NOS have been discovered recently in the genomes of several *Bacillus* species (Kunst et al., 1997), in *S. aureus* (Kuroda et al., 2001), and in *D. radiodurans* (White et al., 1999). We presented here the first detailed characterization of the heme environment of a bacterial NOS in solution.

Heme coordination and spin state of ferric and ferrous SANOS

For the purpose of comparison with the mammalian NOS, the effects of pterin and L-arginine binding on the heme coordination state of ferric and ferrous SANOS were determined. Ferric SANOS, as purified, represents a mixture of 6-coordinate, low-spin and 5-coordinate, high-spin species (Fig. 3, Table 1). Six-coordinate and low-spin ferric forms are observed for $P450_{cam}$, nNOS, and eNOS (Table 1). For the $P450_{cam}$ enzyme, the low-spin species is attributed to a form with a water molecule that is bound to the iron on the distal side of the heme (Poulos et al., 1986). Upon binding of substrate (L-arginine for NOS and camphor for $P450_{cam}$) or cofactor (H_4B in NOS), this water molecule is displaced to give rise to a 5-coordinate and high-spin species (Table 1). Similarly, ferric SANOS is converted into a 5-coordinate and high-spin species upon binding L-arginine or H_4B as shown in the resonance Raman spectra where a single ν_3 line is detected at 1488 cm^{-1} (Table 1). This change of coordination and spin state suggests the existence of a binding site for L-arginine and for a pterin cofactor and that their occupancy by a substrate or a pterin molecule, respectively, prevents the coordination of a water molecule to the iron.

It is noteworthy that ferrous SANOS is 5-coordinate and high-spin, even in the absence of L-arginine and pterin. This is shown by the low frequency of the ν_4 line (1349 cm^{-1}) that is typical of other thiolate-coordinated, 5-coordinate re-

duced heme proteins, and by the frequency of the ν_3 line at 1467 cm^{-1} that is typical of 5-coordinate and high-spin ferrous hemes. Also of interest is the finding that in contrast to mammalian nNOS and iNOS characterized in the absence of the pterin cofactor (Wang et al., 1995), there is no evidence of a 6-coordinate, low-spin form of ferrous SANOS (Fig. 3, *D* and *E*).

The comparison of the CO complexes of SANOS with respect to those of the mammalian NOS

CO is widely used to probe the heme environment of heme proteins. It is particularly sensitive to polar interactions due to the possible electronic delocalization on the Fe-C-O unit (Phillips et al., 1999). It is also sensitive to steric interactions that cause the bending or the tilting of the Fe-C-O unit. We have determined the frequencies of the $\nu_{Fe\text{-}CO}$, $\nu_{C\text{-}O}$, and $\delta_{Fe\text{-}C\text{-}O}$ modes of SANOS. We use these to deduce the properties of the heme pocket and compare them to those of mammalian NOS and P450. First, in the absence of exogenous substrate, we detect two $\nu_{Fe\text{-}CO}$ modes at 482 and 497 cm^{-1}, respectively, and two $\nu_{C\text{-}O}$ modes at 1949 and 1930 cm^{-1}, respectively. This indicates that in SANOS, the CO molecule can adopt two conformations. In nNOS, two conformations of the Fe-C-O unit were observed and assigned to an open conformation, $\nu_{Fe\text{-}CO}$ at 487 cm^{-1} and $\nu_{C\text{-}O}$ at 1949 cm^{-1}, in which the CO molecule is not interacting with neighboring groups, and a closed conformation, with $\nu_{Fe\text{-}CO}$ at 501 cm^{-1} and $\nu_{C\text{-}O}$ at 1930 cm^{-1}, in which a positively charged group interacts with the heme-bound CO molecule (Fan et al., 1997). Similarly, for SANOS, the two conformations can be described as an open conformation where the CO molecule does not interact strongly with neighbor groups, with $\nu_{Fe\text{-}CO}$ at 482 cm^{-1} and $\nu_{C\text{-}O}$ at 1949 cm^{-1}, and a conformation in which a nearby group, positively charged, is interacting with the CO molecule, that give rise to a $\nu_{Fe\text{-}CO}$ mode at 497 cm^{-1} and a $\nu_{C\text{-}O}$ mode at 1930 cm^{-1}. However, upon inspection of the SANOS crystal structure, it does not appear that a positively charged group is present in the vicinity of the heme on the distal side (Bird et al., 2002). It may be that the structure of the ferrous protein in complex with CO differs from that of the ferric enzyme, which is the form crystallized, and that a conformational change occurs upon heme reduction or ligand binding. When plotted on the $\nu_{Fe\text{-}CO}$ versus $\nu_{C\text{-}O}$ correlation graph, the values of the $\nu_{Fe\text{-}CO}$ and $\nu_{C\text{-}O}$ modes of SANOS and SANOS/Arg fall in the region observed for heme proteins having thiolate coordination (Fig. 7, *1–3*). This confirms that the fifth axial ligand of the enzyme in the CO complex is a cysteine residue.

In ferric SANOS, the change in coordination and spin state induced upon binding of L-arginine occurs in the absence of exogenously added pterin, which suggests that SANOS forms a strong complex with L-arginine. This is supported by the finding that the affinity for L-arginine is high, 4.4 ± 0.2 μM (Chartier and Couture, unpublished results), close to the values observed for nNOS (Ghosh et al., 1997). The structure of the heme pocket of SANOS is affected by the binding of L-arginine as observed in the low-frequency region of the resonance Raman spectrum of the CO complex, which displays modifications to several heme modes. Similar to nNOS (Wang et al., 1997) and iNOS (Fan et al., 1997; Li et al., 2004), we observe an increase in the intensity of the modes at 692, 751, and 801 cm^{-1}, respectively, upon L-arginine binding. Recently, Li et al. showed that several modes in the low-frequency region of iNOS in complex with CO and NO are modulated by L-arginine and H_4B binding (Li et al., 2004). These changes were attributed to distortion of the heme imposed by the binding of L-arginine and H_4B (Li et al., 2004). The similarity of the resonance Raman spectra of L-arginine-bound SANOS and that of the mammalian NOS indicate that L-arginine binds in a similar manner in these proteins. The correlation between the modifications to the heme structure, imposed by L-arginine binding, and the catalytic properties of NOS are not known but they may be relevant to the various rates of heme reduction displayed by NOS (Santolini et al., 2001).

In addition to changes to heme modes in the low-frequency region, L-arginine binding caused the replacement of the two $\nu_{Fe\text{-}CO}$ and $\nu_{C\text{-}O}$ modes detected with the L-arginine free enzyme (Table 2) by a single $\nu_{Fe\text{-}CO}$ mode at 504 cm^{-1}.

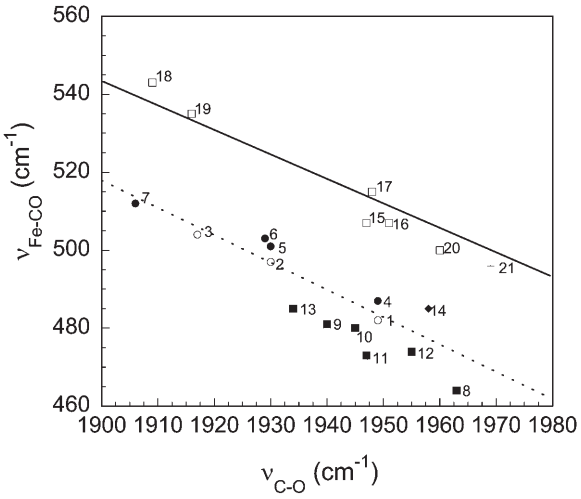

FIGURE 7 Correlation graph of the $\nu_{Fe\text{-}CO}$ and $\nu_{C\text{-}O}$ frequencies for various heme proteins. Identification numbers from 1 to 10 refer to those in Table 2. Frequencies for SANOS (*open circles 1–3*); mammalian nNOS and iNOS (*solid circles 4–7*); $P450_{cam}$ with various substrates (*solid squares 8–13*) (Hu and Kincaid, 1991; Hu et al., 1996); chloroperoxidase, pH 6 (*solid diamond 14*) (Wang et al., 1997); oxygen binding proteins with histidine heme-coordination (*open squares*) including Sperm whale Mb (*15*) (Fuchsman and Appleby, 1979; Ramsden and Spiro, 1989), human HbA (*16*) (Tsubaki et al., 1982), *Ascaris* Hb L and H (*17* and *18*) (Das et al., 2000), *M. tuberculosis* trHbN B and A forms (*19* and *20*) (Yeh et al., 2000), *Bradyrhizobium japonicum* FixL (*21*) (Tomita et al., 2002). The solid line represents the established correlation line for histidine-coordinated heme proteins. The dashed line represents the best correlation line for the mammalian NOS, SANOS, $P450_{cam}$, and chloroperoxidase.

The frequency of the $\nu_{Fe\text{-}CO}$ mode of the L-arginine-bound SANOS complex is similar to that of nNOS/Arg, $\nu_{Fe\text{-}CO}$ at 503 cm^{-1}, but the $\nu_{C\text{-}O}$ frequency differs significantly, 1917 cm^{-1} versus 1929 cm^{-1}, respectively (Table 2). This is more easily observed on the $\nu_{Fe\text{-}CO}$ versus $\nu_{C\text{-}O}$ correlation graph (Fig. 7), where the values for the L-arginine-bound SANOS complex (*open circle 3*) are on the correlation line whereas those of nNOS/Arg are above the correlation line (*solid circle 6*). This observation may be due to a stronger Fe-thiolate bond in SANOS in comparison to the mammalian NOS. Determination of the frequency of the $\nu_{Fe\text{-}Cys}$ mode should reveal whether the strength of the Fe-thiolate bond differs in SANOS as compared to that of eNOS (Schelvis et al., 2002), the only mammalian NOS for which this value has been determined.

The bending mode of the Fe-CO complex is a sensitive indicator of the heme proximal ligand. It is found in the 556–567 cm^{-1} range in P450 and NOS (Table 2), whereas it is in the 577–579 cm^{-1} range in Mb, human Hb, and cytochrome oxidase (Ray et al., 1994). The $\delta_{Fe\text{-}C\text{-}O}$ bending mode of SANOS is detected, with and without substrate, in the range expected from a heme protein with a Fe-thiolate bond (Table 2). Distortion from linearity of the Fe-C-O unit seems to activate the bending mode in some heme proteins. However, distal polar interactions may be even more important, as Ray et al. observed that the intensity of the $\delta_{Fe\text{-}C\text{-}O}$ bending mode is increased by polar interactions in the distal heme pocket and is correlated with significant back-bonding (Ray et al., 1994). That the bending mode is already intense in the absence of substrate in SANOS suggests either that the Fe-C-O unit is distorted from linearity in the substrate-free protein or that a heme pocket group is involved in polar interactions with the CO. Upon L-arginine binding, the bending mode of SANOS becomes more intense and shifts to higher frequency. This shift to higher frequencies is similar to that observed with nNOS and iNOS upon L-arginine binding (Table 2) and it indicates that steric/polar interactions of the CO molecule with L-arginine are similar in these NOS. That strong polar/steric interactions between CO and L-arginine occur in SANOS is also supported by the smaller than expected isotopic shift of the $\nu_{Fe\text{-}CO}$ mode in the presence of L-arginine (8 cm^{-1}, Table 2), as compared to the isotopic shifts in the absence of L-arginine (16 and 12 cm^{-1}, Table 2). This indicates that the CO complex of L-arginine-bound SANOS is not well described by the simple model composed of a two-body oscillator.

Stability of pterin-free SANOS and relation to function

We have shown that ferrous SANOS is totally 5-coordinate and high-spin in the absence of substrate and pterin. We also showed that the CO complex of SANOS is unusually stable in comparison to the CO complex of H_4B-depleted nNOS (Wang et al., 1995) since it shows little change of the absorption spectrum over a 24-h period of incubation at room temperature; the Soret band remained at 445 nm. The band at 445 nm is indicative of the presence of a native structure with thiolate coordination. From the analysis of the primary amino acid sequence and the crystal structure of SANOS (Bird et al., 2002), one might have expected that the protein may have been unstable in the absence of pterin since several residues defining the pterin binding site in mammalian NOS are missing in SANOS, leaving the pterin site more solvent-exposed. This is clearly not the case. Hence, SANOS must have evolved to maintain the structural integrity of the reduced protein in the absence of added cofactor as both the ferrous and ferrous-CO complex are stable with time under these conditions.

That SANOS is stable in the ferrous state without added pterin does not mean that the protein does not require a pterin for its function. With BANOS, it was shown that NO synthesis in single turnover experiments with N^G-hydroxy-L-arginine as the substrate was dependent on the presence of H_4B (Adak et al., 2002a). With DANOS, nitrite formation was stimulated by H_4B in an in vitro assay performed with the reductase domain of nNOS (Adak et al., 2002a). SANOS (F. Chartier and M. Couture, unpublished results), BANOS (Adak et al., 2002a), and DANOS (Adak et al., 2002b) display a slow catalytic rate as determined from the rate of nitrite synthesis under turnover conditions in the presence of the reductase domain of a mammalian NOS. This slow catalytic activity may be related to the use of a pterin that is not the native pterin of bacterial NOS. However, the slow catalytic rates may also result from the use of the reductase domain of a mammalian NOS instead of the native reductase present in the bacteria harboring a NOS gene. Although several N-terminal residues defining the pterin binding site are missing in SANOS and the other bacterial NOS, the crystal structures of SANOS (Bird et al., 2002) and BANOS (Pant et al., 2002) reveal the presence of a cavity corresponding to the H_4B binding site of mammalian NOS. The presence of this cavity and the enhancement of catalytic activity by H_4B suggest that a pterin-like molecule likely binds at this site in the bacterial NOS in vivo. A gene encoding a putative sepiapterin reductase was identified in *B. subtilis* genome by sequence comparison (Kunst et al., 1997). Sequence data bank search with sepiapterin reductase sequences are not conclusive about the presence of a similar gene in *S. aureus* (F. Chartier and M. Couture, unpublished results). Little is known about the pathways for pterin biosynthesis in bacteria harboring a NOS gene, and clearly, more studies are required to determine the nature of the native cofactor of bacterial NOS.

CONCLUSIONS

SANOS responds to the binding of L-arginine in a manner similar to that observed for mammalian NOS both in the ferric and CO states. However, the behavior of the enzyme

with respect to pterin is remarkable. First, although binding of H_4B or THF changed the spin state and coordination state of the heme iron in the ferric form, these molecules are not required for the maintenance of the ferrous protein in the 5-coordinate and high-spin state. Second, the CO complex does not degrade over time to a P420-like form in the absence of added pterin. Third, a spectral signature for the binding of H_4B or THF in the CO complex was observed only in combination with L-arginine, suggesting that the effects of H_4B and THF binding to the CO complex are modest. Altogether, these results suggest that although a pterin is probably required for catalysis by SANOS, through electron/proton transfer, it may not have a structural role as in mammalian NOS, where the pterin cofactor is required to maintain the ferrous heme in the 5-coordinate and high-spin state and to prevent the conversion of the enzyme to the P420-like form.

This work was supported by the National Sciences and Engineering Research Council of Canada grant 250073, Canadian Foundation for Innovation equipment grant 7128, and the Fonds Québécois de la Recherche sur la Nature et les Technologies grant 78927 to M.C.

REFERENCES

Abu-Soud, H. M., M. Loftus, and D. J. Stuehr. 1995. Subunit dissociation and unfolding of macrophage NO synthase: relationship between enzyme structure, prosthetic group binding, and catalytic function. *Biochemistry*. 34:11167–11175.

Adak, S., K. S. Aulak, and D. J. Stuehr. 2002a. Direct evidence for nitric oxide production by a nitric-oxide synthase-like protein from *Bacillus subtilis*. *J. Biol. Chem.* 277:16167–16171.

Adak, S., A. M. Bilwes, K. Panda, D. Hosfield, K. S. Aulak, J. F. McDonald, J. A. Tainer, E. D. Getzoff, B. R. Crane, and D. J. Stuehr. 2002b. Cloning, expression, and characterization of a nitric oxide synthase protein from *Deinococcus radiodurans*. *Proc. Natl. Acad. Sci. USA*. 99:107–112.

Adak, S., Q. Wang, and D. J. Stuehr. 2000. Arginine conversion to nitroxide by tetrahydrobiopterin-free neuronal nitric-oxide synthase. Implications for mechanism. *J. Biol. Chem.* 275:33554–33561.

Alderton, W. K., C. E. Cooper, and R. G. Knowles. 2001. Nitric oxide synthases: structure, function and inhibition. *Biochem. J.* 357:593–615.

Aono, S., T. Kato, M. Matsuki, H. Nakajima, T. Ohta, T. Uchida, and T. Kitagawa. 2002. Resonance Raman and ligand binding studies of the oxygen-sensing signal transducer protein HemAT from *Bacillus subtilis*. *J. Biol. Chem.* 277:13528–13538.

Appleby, C. A. 1978. Purification of Rhizobium cytochromes P-450. *Methods Enzymol.* 52:157–166.

Bird, L. E., J. Ren, J. Zhang, N. Foxwell, A. R. Hawkins, I. G. Charles, and D. K. Stammers. 2002. Crystal structure of SANOS, a bacterial nitric oxide synthase oxygenase protein from *Staphylococcus aureus*. *Structure (Camb).* 10:1687–1696.

Champion, P. M., I. C. Gunsalus, and G. C. Wagner. 1978. Resonance Raman investigations of cytochrome P450cam from *Pseudomonas putida*. *J. Am. Chem. Soc.* 100:3743–3751.

Chen, Y., and J. P. Rosazza. 1994. A bacterial nitric oxide synthase from a *Nocardia* species. *Biochem. Biophys. Res. Commun.* 203:1251–1258.

Chen, Y., and J. P. N. Rosazza. 1995. Purification and characterization of nitric oxide synthase (NOS_{NOC}) from *Nocardia* species. *J. Bacteriol.* 177:5122–5128.

Cosentino, F., and T. F. Luscher. 1999. Tetrahydrobiopterin and endothelial nitric oxide synthase activity. *Cardiovasc. Res.* 43:274–278.

Couture, M., T. Burmester, T. Hankeln, and D. L. Rousseau. 2001. The heme environment of mouse neuroglobin. Evidence for the presence of two conformations of the heme pocket. *J. Biol. Chem.* 276:36377–36382.

Das, T. K., J. M. Friedman, A. P. Kloek, D. E. Goldberg, and D. L. Rousseau. 2000. Origin of the anomalous Fe-CO stretching mode in the CO complex of *Ascaris* hemoglobin. *Biochemistry*. 39:837–842.

Fan, B., J. Wang, D. J. Stuehr, and D. L. Rousseau. 1997. NO synthase isozymes have distinct substrate binding sites. *Biochemistry*. 36:12660–12665.

Fuchsman, W. H., and C. A. Appleby. 1979. CO and O_2 complexes of soybean leghemoglobins: pH effects upon infrared and visible spectra. Comparisons with CO and O_2 complexes of myoglobin and hemoglobin. *Biochemistry*. 18:1309–1321.

Ghosh, D. K., C. Wu, E. Pitters, M. Moloney, E. R. Werner, B. Mayer, and D. J. Stuehr. 1997. Characterization of the inducible nitric oxide synthase oxygenase domain identifies a 49 amino acid segment required for subunit dimerization and tetrahydrobiopterin interaction. *Biochemistry*. 36:10609–10619.

Hu, S., and J. R. Kincaid. 1991. Resonance Raman characterization of nitric oxide adducts of cytochrome P450cam: the effect of substrate structure on the iron-ligand vibrations. *J. Am. Chem. Soc.* 113:2843–2850.

Hu, S., K. M. Smith, and T. G. Spiro. 1996. Assignment of protoheme resonance Raman spectrum by heme labeling in myoglobin. *J. Am. Chem. Soc.* 118:12638–12646.

Igarashi, J., A. Sato, T. Kitagawa, I. Sagami, and T. Shimizu. 2003. CO binding study of mouse heme-regulated eIF-2alpha kinase: kinetics and resonance Raman spectra. *Biochim. Biophys. Acta.* 1650:99–104.

Kunst, F., N. Ogasawara, I. Moszer, A. M. Albertini, G. Alloni, V. Azevedo, M. G., Bertero, P. Bessieres, A. Bolotin, S. Borchert, et al. 1997. The complete genome sequence of the gram-positive bacterium *Bacillus subtilis*. *Nature*. 390:249–256.

Kuroda, M., T. Ohta, I. Uchiyama, T. Baba, H. Yuzawa, I. Kobayashi, L. Cui, A. Oguchi, K. Aoki, Y. Nagai, and others. 2001. Whole genome sequencing of meticillin-resistant *Staphylococcus aureus*. *Lancet*. 357:1225–40.

Li, D., D. J. Stuehr, S. R. Yeh, and D. L. Rousseau. 2004. Heme distortion modulated by ligand-protein interactions in inducible nitric oxide synthase. *J. Biol. Chem.* 279:26489–26499.

Li, X.-Y., and T. G. Spiro. 1988. Is bound CO linear or bent in heme proteins? Evidence from resonance Raman and infrared spectroscopic data. *J. Am. Chem. Soc.* 110:6024–6033.

Marletta, M. A. 1994. Nitric oxide synthase: aspects concerning structure and catalysis. *Cell*. 78:927–930.

McMillan, K., and B. S. Masters. 1993. Optical difference spectrophotometry as a probe of rat brain nitric oxide synthase heme-substrate interaction. *Biochemistry*. 32:9875–9880.

Mukai, M., P. Y. Savard, H. Ouellet, M. Guertin, and S. R. Yeh. 2002. Unique ligand-protein interactions in a new truncated hemoglobin from *Mycobacterium tuberculosis*. *Biochemistry*. 41:3897–3905.

Pant, K., A. M. Bilwes, S. Adak, D. J. Stuehr, and B. R. Crane. 2002. Structure of a nitric oxide synthase heme protein from *Bacillus subtilis*. *Biochemistry*. 41:11071–11079.

Phillips, G. N. J., M. L. Teodoro, T. Li, B. Smith, and J. S. Olson. 1999. Bound CO is a molecular probe of electrostatic potential in the distal pocket of myoglobin. *J. Phys. Chem. B*. 103:8817–8829.

Poulos, T. L., B. C. Finzel, and A. J. Howard. 1986. Crystal structure of substrate-free *Pseudomonas putida* cytochrome P-450. *Biochemistry*. 25:5314–5322.

Raman, C. S., P. Martasek, and B. S. S. Masters. 2000. Structural themes determining function in nitric oxide synthases. *In* The Porphyrin Handbook. K. M. Kadish, K. M. Smith, and R. Guilard, editors. Academic Press, New York. 293–339 p.

Ramsden, J., and T. G. Spiro. 1989. Resonance Raman evidence that distal histidine protonation removes the steric hindrance to upright binding of carbon monoxide by myoglobin. *Biochemistry.* 28:3125–3128.

Ray, G. B., X.-Y. Li, J. A. Ibers, J. L. Sessler, and T. G. Spiro. 1994. How far can proteins bend the FeCO unit? Distal polar and steric effects in heme proteins and models. *J. Am. Chem. Soc.* 116:162–176.

Rodriguez-Crespo, I., P. Moenne-Loccoz, T. M. Loehr, and P. R. Ortiz de Montellano. 1997. Endothelial nitric oxide synthase: modulations of the distal heme site produced by progressive N-terminal deletions. *Biochemistry.* 36:8530–8538.

Sambrook, J., E. F. Fritsch, and T. Maniatis. 1989. Molecular Cloning: A Laboratory Manual, 2nd ed. Cold Spring Harbor Laboratory Press, Cold Spring Harbor, NY.

Santolini, J., A. L. Meade, and D. J. Stuehr. 2001. Differences in three kinetic parameters underpin the unique catalytic profiles of nitric-oxide synthases I, II, and III. *J. Biol. Chem.* 276:48887–48898.

Schelvis, J. P., V. Berka, G. T. Babcock, and A. L. Tsai. 2002. Resonance Raman detection of the Fe-S bond in endothelial nitric oxide synthase. *Biochemistry.* 41:5695–5701.

Sengupta, R., R. Sahoo, S. Mukherjee, M. Regulski, T. Tully, D. J. Stuehr, and S. Ghosh. 2003. Characterization of Drosophila nitric oxide synthase: a biochemical study. *Biochem. Biophys. Res. Commun.* 306:590–597.

Spiro, T. G., and X. Y. Li. 1988. Resonance Raman spectroscopy of metalloproteins. *In* Biological Applications of Raman Spectroscopy. T. G. Spiro, editor. John Wiley, New York. 39–96.

Tomita, T., G. Gonzalez, A. L. Chang, M. Ikeda-Saito, and M. A. Gilles-Gonzalez. 2002. A comparative resonance Raman analysis of heme-binding PAS domains: heme iron coordination structures of the BjFixL, AxPDEA1, EcDos, and MtDos proteins. *Biochemistry.* 41:4819–4826.

Tsubaki, M., R. B. Srivastava, and N. T. Yu. 1982. Resonance Raman investigation of carbon monoxide bonding in (carbon monoxy)hemoglobin and -myoglobin: detection of Fe-CO stretching and Fe-C-O bending vibrations and influence of the quaternary structure change. *Biochemistry.* 21:1132–1140.

Uchida, T., H. Ishikawa, S. Takahashi, K. Ishimori, I. Morishima, K. Ohkubo, H. Nakajima, and S. Aono. 1998. Heme environmental structure of CooA is modulated by the target DNA binding. Evidence from resonance Raman spectroscopy and CO rebinding kinetics. *J. Biol. Chem.* 273:19988–19992.

Uno, T., Y. Nishimura, R. Makino, T. Iizuka, Y. Ishimura, and M. Tsuboi. 1985. The resonance Raman frequencies of the Fe-CO stretching and bending modes in the CO complex of cytochrome P-450cam. *J. Biol. Chem.* 260:2023–2026.

Vogel, K. M., P. M. Kozlowski, M. Z. Zgierski, and T. G. Spiro. 2000. Role of the axial ligand in heme-CO backbonding; DFT analysis of vibrational data. *Inorg. Chim. Acta.* 297:11–17.

Wang, J., W. S. Caughey, and D. L. Rousseau. 1996. Resonance Raman scattering: a probe of heme protein-bound nitric oxide. *In* Methods in Nitric Oxide Research. M. Feelish and J. S. Stamler, editors. John Wiley & Sons, New York.

Wang, J., D. J. Stuehr, M. Ikeda-Saito, and D. L. Rousseau. 1993. Heme coordination and structure of the catalytic site in nitric oxide synthase. *J. Biol. Chem.* 268:22255–22258.

Wang, J., D. J. Stuehr, and D. L. Rousseau. 1995. Tetrahydrobiopterin-deficient nitric oxide synthase has a modified heme environment and forms a cytochrome P-420 analogue. *Biochemistry.* 34:7080–7087.

Wang, J., D. J. Stuehr, and D. L. Rousseau. 1997. Interactions between substrate analogues and heme ligands in nitric oxide synthase. *Biochemistry.* 36:4595–4606.

Wei, C. C., B. R. Crane, and D. J. Stuehr. 2003. Tetrahydrobiopterin radical enzymology. *Chem. Rev.* 103:2365–2383.

Wells, A. V., P. Li, P. M. Champion, S. A. Martinis, and S. G. Sligar. 1992. Resonance Raman investigations of *Escherichia coli*-expressed *Pseudomonas putida* cytochrome P450 and P420. *Biochemistry.* 31:4384–4393.

White, O., J. A. Eisen, J. F. Heidelberg, E. K. Hickey, J. D. Peterson, R. J. Dodson, D. H. Haft, M. L. Gwinn, W. C. Nelson, D. L. Richardson, et al. 1999. Genome sequence of the radioresistant bacterium *Deinococcus radiodurans* R1. *Science.* 286:1571–1577.

Yeh, S. R., M. Couture, Y. Ouellet, M. Guertin, and D. L. Rousseau. 2000. A cooperative oxygen binding hemoglobin from *Mycobacterium tuberculosis.* Stabilization of heme ligands by a distal tyrosine residue. *J. Biol. Chem.* 275:1679–1684.

Yu, N. T., B. Benko, E. A. Kerr, and K. Gersonde. 1984. Iron-carbon bond lengths in carbonmonoxy and cyanomet complexes of the monomeric hemoglobin III from *Chironomus thummi thummi*: a critical comparison between resonance Raman and x-ray diffraction studies. *Proc. Natl. Acad. Sci. USA.* 81:5106–5110.